

Localization Driven Superradiant Instability

Honghao Yin,¹ Jie Hu,¹ An-Chun Ji,^{1,*} Gediminas Juzeliūnas^{2,†}, Xiong-Jun Liu^{3,4,5,6,‡} and Qing Sun^{1,§}

¹*Department of Physics, Capital Normal University, Beijing 100048, China*

²*Institute of Theoretical Physics and Astronomy, Vilnius University, Saulėtekio 3, LT-10257 Vilnius, Lithuania*

³*International Center for Quantum Materials, School of Physics, Peking University, Beijing 100871, China*

⁴*Beijing Academy of Quantum Information Science, Beijing 100193, China*

⁵*CAS Center for Excellence in Topological Quantum Computation, University of Chinese Academy of Sciences, Beijing 100190, China*

⁶*Institute for Quantum Science and Engineering and Department of Physics, Southern University of Science and Technology, Shenzhen 518055, China*



(Received 16 September 2019; accepted 24 February 2020; published 17 March 2020)

The prominent Dicke superradiant phase arises from coupling an ensemble of atoms to a cavity optical field when an external optical pumping exceeds a threshold strength. Here we report a prediction of the superradiant instability driven by Anderson localization, realized with a hybrid system of the Dicke and Aubry-André (DAA) model for bosons trapped in a one-dimensional (1D) quasiperiodic optical lattice and coupled to a cavity. Our central finding is that for bosons condensed in a localized phase given by the DAA model, the resonant superradiant scattering is induced, for which the critical optical pumping of the superradiant phase transition approaches zero, giving an instability driven by the Anderson localization. The superradiant phase for the DAA model with or without a mobility edge is investigated, showing that the localization driven superradiant instability is in sharp contrast to the superradiance as widely observed for a Bose-Einstein condensate in extended states, and should be insensitive to the temperature of the system. This study unveils a novel effect of localization on the Dicke superradiance, and is well accessible based on the current experiments.

DOI: [10.1103/PhysRevLett.124.113601](https://doi.org/10.1103/PhysRevLett.124.113601)

Combining cold atomic gases with the cavity quantum electrodynamics [1–9] has provided a unique platform to explore exotic quantum states in atom-cavity coupling systems [10–21]. In particular, the cavity field mediates an effective long-range interaction between all atoms, and a prominent superradiant phase with the atoms absorbing and emitting the photons collectively was predicted in the notable Dicke model [22,23]. Such superradiance transition has been achieved dynamically with a Bose-Einstein condensate (BEC) coupled to a transversely pumped optical cavity [24–29]. Furthermore, for degenerate Fermi gases inside a cavity, the superradiance with enhancement by the Fermi surface nesting was predicted [30–32], and further the topological superradiant phases were also proposed [33,34]. These studies reveal the strong correlations between cavity photons and external center-of-mass (c.m.) motion of atomic assembles in the dispersive coupling regime [8], with many exotic nonequilibrium quantum behaviors having been uncovered in these open systems [35–40].

The emergence of the superradiance for BECs in a cavity is typically associated with the formation of a self-organized supersolid [24,25]. The disordered potential, if applied to the atoms, is expected to have significant effect on the superradiance. In particular, the cavity-induced incommensurate lattice can induce the Bose-glass phases in a Bose-Hubbard system as the optical pumping is strong enough

[41], affect localization transition of the atomic c.m. [42,43], and lead to anomalous diffusion of the atomic wave packets [44]. In these studies, the atoms are in ordered or extended states before the superradiance occurs. A question is, what happens if considering the coupling of an initially localized phase to cavity?

In this Letter, we investigate a BEC in a localized phase given by a one-dimensional quasiperiodical superlattice potential and coupled to a transversely pumped optical cavity, the latter providing an effective long range interaction between the atoms. The incommensurate quasiperiodical potential can lead to the Anderson localization [45–56] and the many-body localization which has attracted a considerable amount of interest recently [57–60]. In the extended regime, increasing the strength of the incommensurate potential can facilitate the tendency to the superradiant phase. Surprisingly, when the atoms enter the localized phase, we show that an unprecedented superradiant instability is driven by the resonant superradiant scatterings, for which the superradiance occurs at an arbitrarily small optical pumping strength.

We consider a BEC inside a high-finesse optical cavity along the x direction (Fig. 1). The atoms experience a one-dimensional (1D) static bichromatic incommensurate potential $V_{\text{static}}(x) = V_1 \cos^2(k_1 x) + V_2 \cos^2(k_2 x + \phi)$ obtained by superimposing two optical lattices, with ϕ a tunable

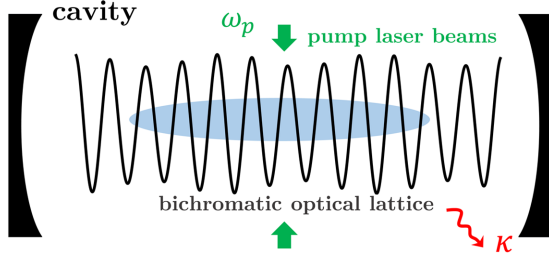


FIG. 1. A schematic diagram of the system. A 1D BEC is placed inside a high-finesse optical cavity and driven by pump laser beams counterpropagating along the z direction. The atoms are subjected to a 1D static bichromatic potential along the x direction, and the transverse motion of atoms is suppressed by a large transverse confinement.

relative phase, and are also illuminated by a standing-wave pumping laser with the frequency ω_p in the z direction. The transverse motion is suppressed by a strong confinement. In the rotating frame, the Hamiltonian reads $\hat{\mathcal{H}} = \int dx \hat{\psi}^\dagger(x) \hat{H} \hat{\psi}(x) - \hbar \Delta_c \hat{a}^\dagger \hat{a}$, where $\Delta_c = \omega_p - \omega_c$ is the detuning between the pumping laser and the cavity field, $\hat{\psi}(x)$ and \hat{a} are the annihilation operators of the atom and cavity photon, respectively. The full Hamiltonian reads $\hat{H} = \hat{H}_0 + V_{\text{dynamic}}(x)$ [20], with $\hat{H}_0 = -(\hbar^2/2m)\nabla^2 + V_{\text{static}}(x)$. Here $V_{\text{dynamic}}(x) = \hbar\eta(\hat{a}^\dagger + \hat{a})\cos(k_c x) + \hbar U \hat{a}^\dagger \hat{a} \cos^2(k_c x)$ is the cavity-assisted potential, m is the atom mass, and $\eta = \eta_0 \cos(k_p z_0)$ is the pumping amplitude, with $\eta_0 = g\Omega/\Delta_a$ being the strength of the interference between the pumping laser and the cavity field. Here also $U = g^2/\Delta_a$ is the dispersive coupling strength, $\Delta_a = \omega_p - \omega_a$ is the detuning of pumping laser to atomic transition frequency ω_a , and Ω (g) is the (single-photon) Rabi frequency of the pumping laser (cavity mode). In this Letter we focus on the superradiant instability with weak pumping and cavity fields, and the tight-binding model for the following study can be developed based on the atomic Wannier basis of the static lattice [20,39,40].

To better understand the model, we analyze first the situation without the pumping laser and the cavity field. We choose $V_1 \cos^2(k_1 x)$ ($V_1 > V_2$) as the primary lattice, and the secondary lattice $V_2 \cos^2(k_2 x)$ is relatively weaker. In the tight-binding limit, the atomic Hamiltonian $\hat{\mathcal{H}}_0$ for the bichromatic potential can be cast in the form of the Aubry-André (AA) model [45]

$$\hat{\mathcal{H}}_{\text{AA}} = -J \sum_j (\hat{c}_j^\dagger \hat{c}_{j+1} + \text{H.c.}) + \chi \sum_j \cos(2\pi\gamma j) \hat{c}_j^\dagger \hat{c}_j, \quad (1)$$

where J is the nearest-neighbor tunneling and the quasirandom disorder is induced by an additional incommensurate lattice, characterized by the ratio of the lattice wave numbers $\gamma = k_2/k_1$ and disorder strength χ . For the maximally incommensurate ratio $\gamma = (\sqrt{5} - 1)/2$, the model

undergoes an Anderson transition from extended to localized states at $\chi/J = 2$, beyond which all the states are localized. Such a transition has been well observed for noninteracting BECs [46,47] and photonic crystals [48]. Beyond the tight-binding limit, corrections are added to the AA model, leading to a general Aubry-André (GAA) model Hamiltonian $\hat{\mathcal{H}}_{\text{GAA}} = \hat{\mathcal{H}}_{\text{AA}} + \hat{\mathcal{H}}'$, with

$$\begin{aligned} \hat{\mathcal{H}}' = & J_2 \sum_j (\hat{c}_j^\dagger \hat{c}_{j+2} + \text{H.c.}) + \chi' \sum_j \cos(4\pi\gamma j) \hat{c}_j^\dagger \hat{c}_j \\ & + J' \sum_j \cos\left[2\pi\gamma\left(j + \frac{1}{2}\right)\right] (\hat{c}_j^\dagger \hat{c}_{j+1} + \text{H.c.}), \quad (2) \end{aligned}$$

where J_2 is the next-nearest-neighbor (NNN) hopping amplitude, J' and χ' are the correction parameters to the tunneling parameter J and disorder strength χ , respectively. Unlike the AA model, the GAA model may have an intermediate phase, where the localized and extended eigenstates can coexist and are separated by a single-particle mobility edge (SPME) [60].

The present system represents a hybrid Dicke and Aubry-André (DAA) model, characterizing BEC in the quasiperiodic lattice and coupled to the cavity. The dynamics is captured by a master equation $\dot{\rho} = -i[\hat{\mathcal{H}}, \rho] + \mathcal{L}\rho$ on the density matrix ρ and studied self-consistently, where the DAA Hamiltonian $\hat{\mathcal{H}} = \hat{\mathcal{H}}_{\text{AA/GAA}} - \Delta_c \hat{a}^\dagger \hat{a} + \eta(\hat{a}^\dagger + \hat{a}) \times \sum_j \cos(2\pi\gamma_c j) \hat{c}_j^\dagger \hat{c}_j + U \hat{a}^\dagger \hat{a} \sum_j \cos^2(2\pi\gamma_c j) \hat{c}_j^\dagger \hat{c}_j$, and $\mathcal{L}\rho = \kappa(2\hat{a}\rho\hat{a}^\dagger - \hat{a}^\dagger\hat{a}\rho - \rho\hat{a}^\dagger\hat{a})$ is a Lindblad term to describe the cavity loss with a decay rate κ . Replacing the cavity field operator \hat{a} by a c number $a \equiv \langle \hat{a} \rangle$ yields $i\partial_t a = [-\Delta_c - i\kappa + U \sum_j \cos^2(2\pi\gamma_c j) \langle \hat{c}_j^\dagger \hat{c}_j \rangle] a + \eta \sum_j \cos(2\pi\gamma_c j) \langle \hat{c}_j^\dagger \hat{c}_j \rangle$, where $\gamma_c = k_c/2k_1$ and $\langle \hat{c}_j^\dagger \hat{c}_j \rangle$ is the atomic density distribution. By setting $\partial_t a = 0$, the steady-state solution reads

$$a = - \frac{\eta \sum_j \cos(2\pi\gamma_c j) \langle \hat{c}_j^\dagger \hat{c}_j \rangle}{-\Delta_c - i\kappa + U \sum_j \cos^2(2\pi\gamma_c j) \langle \hat{c}_j^\dagger \hat{c}_j \rangle}. \quad (3)$$

Note that $\langle \hat{c}_j^\dagger \hat{c}_j \rangle$ itself depends on the cavity-assisted potential, and should be determined self-consistently. In general, one can expect a transition from a “normal” state with $a = 0$ to a “superradiant” state with $a \neq 0$ by tuning, e.g., the optical pumping strength η .

Figure 2 shows the numerical results of the critical pumping strength η_c versus the eigenstate of the DAA Hamiltonian $\hat{\mathcal{H}}$ with energy ϵ_α . For the GAA model, an intermediate phase with a SPME for $\chi/J = 2.1$ is given around the energy $\epsilon_c/J \simeq 0.44$. The inverse participation ratio $\text{IPR}^{(\alpha)} \equiv \sum_j |\phi_j^\alpha|^4 / (\sum_j |\phi_j^\alpha|^2)^2$ vanishes for extended states and becomes finite for localized states across the SPME (inset of Fig. 2). For the AA model, as $\chi/J > 2$, the system is in the localization phase with all the eigenstates being localized.

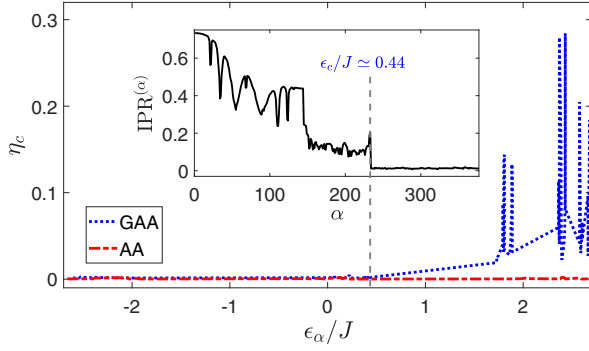


FIG. 2. The critical pumping strength η_c as a function of the energy ϵ_α/J for atoms in different eigenstates at the disorder strength $\chi/J = 2.1$ for the DAA model. The inset shows the inverse participation ratio (IPR) of the eigenstates in the GAA model with a SPME ($\alpha \sim 233$ marked by vertical dashed line). We have chosen $U/J = 0.1$, $J'/J = -0.23$, $J_2/J = 0.072$, $\chi'/J = -0.016$. Other parameters are $\gamma = 233/377 \approx 0.618$, $\gamma_c = 0.8$, and $L = 377$ for the numerical calculation.

Our key observation is that an unprecedented localization driven superradiant instability is obtained, i.e., the cavity field emerges spontaneously for an arbitrarily small pumping strength. More exactly, whenever the BEC is in a localized state, no matter the ground state or an excited one, the superradiance takes place at a vanishing critical pumping strength. This is in sharp contrast to the extended state, where a finite pumping strength is generally required [24–28] (see also the blue-dotted line of the GAA model in Fig. 2). Since all states in the AA model with $\chi/J > 2$ are localized and not thermalizable, the superradiant instability can be obtained for the BEC with any energy within the localized band, implying that this result is insensitive to the temperature.

To gain a deeper insight to the underlying physics, we analyze the superradiant behavior as the atomic wave function undergoes the delocalization-to-localization transition. We take the AA model for illustration. Diagonalizing the Hamiltonian (1), we have $\hat{\mathcal{H}}_0 = \sum_\alpha \epsilon_\alpha \hat{c}_\alpha^\dagger \hat{c}_\alpha$, with ϵ_α and $\hat{c}_\alpha = \sum_j \hat{c}_j \phi_\alpha^j$ being, respectively, the eigenenergy and the annihilation operator of the corresponding eigenstate ϕ_α . The total Hamiltonian of the system can then be rewritten as

$$\begin{aligned} \hat{\mathcal{H}} = & \sum_\alpha \epsilon'_\alpha \hat{c}_\alpha^\dagger \hat{c}_\alpha + \eta (\hat{a}^\dagger + \hat{a}) \sum_{\alpha\beta} (s_{\alpha\beta} \hat{c}_\alpha^\dagger \hat{c}_\beta + \text{H.c.}) \\ & + U \hat{a}^\dagger \hat{a} \sum_{\alpha\beta} (h_{\alpha\beta} \hat{c}_\alpha^\dagger \hat{c}_\beta + \text{H.c.}) - \Delta_c \hat{a}^\dagger \hat{a}, \end{aligned} \quad (4)$$

which leads to a series of coupled equations of motion

$$\begin{aligned} i\dot{a} = & -ika - \Delta_c a + Ua \sum_{\alpha\beta} (h_{\alpha\beta} c_\alpha^* c_\beta + \text{H.c.}) \\ & + \eta \sum_{\alpha\beta} (s_{\alpha\beta} c_\alpha^* c_\beta + \text{H.c.}), \end{aligned} \quad (5)$$

$$i\dot{c}_\alpha = \epsilon'_\alpha c_\alpha + \eta (a^* + a) \sum_\beta s_{\alpha\beta} c_\beta + U|a|^2 \sum_\beta h_{\alpha\beta} c_\beta. \quad (6)$$

Here $\epsilon'_\alpha \equiv \epsilon_\alpha - \epsilon_0$ is the eigenenergy measured from the lowest one ($\alpha = 0$), $s_{\alpha\beta} \equiv \sum_j \phi_\alpha^{j*} \cos(2\pi\gamma_c j) \phi_\beta^j$ and $h_{\alpha\beta} \equiv \sum_j \phi_\alpha^{j*} \cos^2(2\pi\gamma_c j) \phi_\beta^j$ denote the scatterings between α and β states. For the superradiant transition, we take that the atoms are condensed in the lowest state $\alpha = 0$, and are weakly scattered to other states when the cavity field emerges. In this case only the scattering terms $s_{0\alpha}$ and $h_{0\alpha}$ are relevant. We define for convenience $s_\alpha \equiv s_{0\alpha} = s_{\alpha 0}^*$ and $h_\alpha \equiv h_{0\alpha} = h_{\alpha 0}^*$. The case for atoms initially condensed in other states is similar.

Let us now examine the superradiance phase transition. When $\chi/J < 2$, the states are extended, resembling the quasimomentum states. One finds that the cavity field cannot induce self-scattering within the ground state and so $s_0 = 0$. The critical value of the pumping field reads

$$\eta_c = \sqrt{\frac{1}{4Nf_1} \frac{\kappa^2 + \bar{\Delta}'_c}{-\bar{\Delta}'_c}}, \quad (7)$$

with $f_1 = \sum_\alpha |s_\alpha|^2 / \epsilon'_\alpha$, $\bar{\Delta}'_c = \Delta_c - UNh_0$, where $h_0 = 1/2$ gives a constant shift of cavity detuning. In the extended regime, the susceptibility f_1 is finite and the critical value of the pumping strength determined by Eq. (7) is also finite. On the other hand, Fig. 3(a) shows that as the disorder strength increases, the value f_1 increases rapidly (red curve), and the superradiance tendency is strongly enhanced, with the critical pumping field strength η_c (blue curve) decreasing significantly with an increase of the disorder in the lattice potential. When increasing χ to the delocalization-to-localization transition point with $\chi/J = 2$, the susceptibility f_1 diverges and the superradiance threshold becomes zero.

The unique role played by the incommensurate lattice potential on the superradiance enhancement becomes more transparent in the momentum space. For the limit case with $\chi = 0$ (no disorder lattice), the momentum distribution of the ground state, $P(k/k_1) = |\sum_j \phi_0^j \exp(i\pi j k/k_1)|^2$, exhibits primary peaks at $k = 0$ and $2k_1$ (equivalent to $-2k_1$) in the first Brillouin zone [47–51]. The momentum peaks of the α th excited state are found to appear at $\pm \alpha k_1/L$ and $\pm(2 - \alpha/L)k_1$, which are shifted from the primary peaks of the ground state by $\pm \alpha k_1/L$, with α being integers, as shown in Fig. 3(b). Note that the pumping laser and the cavity field excite the atoms from the ground state to the excited states. The scattering to the α th state contributes to the susceptibility $f_1^\alpha \equiv |s_\alpha|^2 / \epsilon'_\alpha$. A cavity photon carries a momentum k_c , so only the α_0 th state with $\alpha_0 = 2L(1 - \gamma_c)$ that matches the cavity mode can be excited, giving a lattice version of the Dicke model for the noninteracting Bose gas.

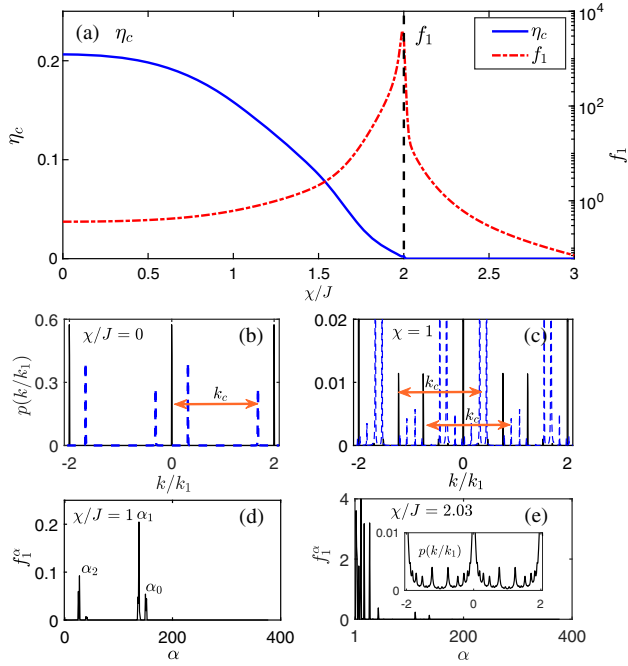


FIG. 3. (a) The critical pumping field strength η_c and the susceptibility f_1 as a function of the disorder strength χ/J for $L = 377$, $N = 100$, $\Delta_c/J = -1$, $\kappa/J = 1$, and $\gamma_c = 4/5$. The momentum distributions of the ground state (black solid) and excited state (blue dashed) with disorder strength $\chi/J = 0.0$ (b) and 1.0 (c). Susceptibility f_1^α for the disorder strength $\chi/J = 1$ (d) and $\chi/J = 2.03$ (e). In the latter the term f_1^0 diverges and is not plotted. The inset shows the corresponding momentum distribution of the ground state.

When the secondary lattice is added, the momentum distributions of the eigenstates are modified with the appearance of new peaks. For the ground state, additional peaks $\pm 2(k_1 - k_2)$, $\pm 2k_2$ occur between the primary peaks. Accordingly, we show that new momentum peaks of the excited states appear around the peaks of the ground state within the distance $\alpha k_1/L$, see the dashed lines in Fig. 3(c). In this case, besides the α_0 th state, we find two new excited states that take part in the atom-light scattering process, with $\alpha_1 = 2L(\gamma_c - \gamma)$ and $\alpha_2 = 2L(\gamma_c + 2\gamma - 2)$, see Fig. 3(d). Compared to the α_1 th state, which is a higher-excited state near the α_0 th state, the α_2 th state is located near the low-energy excitation regime, and can dominate the contribution to the susceptibility. As the incommensurate lattice potential increases, more and more peaks arise in the momentum distributions of the ground and excited states, enhancing the contribution to the susceptibility and decreasing the critical pumping of the superradiant transition.

The nontrivial transition is obtained as the disorder strength χ/J approaches 2, beyond which the eigenstates become localized in the real space, but extended in the momentum space, namely, the momentum distribution of each state spans the whole momentum space [see the inset

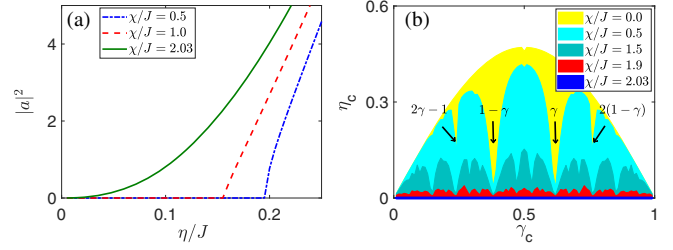


FIG. 4. (a) The steady-state photon number $|a|^2$ as a function of η/J for $\chi/J = 0.5$ (blue dash-dotted), 1.0 (red dashed), and 2.03 (green solid). (b) The diagram of the critical coupling strength η_c versus γ_c for different χ . Here, the parameters are $L = 377$, $N = 100$, $\Delta_c/J = -1$, and $\kappa/J = 1$.

of Fig. 3(e) for a reference]. In such a situation, each localized state can be scattered to itself by the cavity field via inducing transition between different momentum components within the state. This gives rise to the resonant superradiant scattering. Consequently the susceptibility $f_1 = \sum_\alpha f_1^\alpha$ diverges due to the contribution from the resonant self-scattering term f_1^0 , for which the threshold pumping strength vanishes, as shown in Fig. 3(a). The direct calculation shows that $s_{\alpha\alpha}$ is finite for any excited localized state as $\chi/J > 2$ and approaches $\cos(2\pi\gamma_c j_l)$ in the deep localized regime, where j_l is the central site of the localized wave function. Thus the superradiant instability is achieved for the whole localized band.

The predicted superradiant instability can be understood by a symmetry argument. For the conventional self-organization superradiant transition of the BEC, a finite critical pumping is necessary to break both the Z_2 and translational symmetries [20,24,35–37]. In the present superradiant instability, where the translational symmetry is already absent for the localization phase, the superradiant transition only breaks the Z_2 symmetry. The absence of the translational symmetry breaking accounts for the vanishing of the critical pumping [61].

The present prediction can be readily observed in experiments by monitoring the photon number [24] versus coupling strength η for different disorder χ . Figure 4(a) shows that the cavity photons emerge with a very small pumping field, suggesting a vanishing critical coupling. Moreover, the value η_c depends on the wave vector (characterized by γ_c) of cavity field, as shown in Fig. 4(b) for different χ . When γ_c matches the disorder potential, i.e., $\gamma_c \sim n\gamma$ or $n(1 - \gamma)$, with n being a positive integer [see the arrows in 4(b)], the cavity field enhances the disorder potential and the critical pumping strength drops more quickly versus χ . Finally, we found that the predicted superradiant instability has no finite-size effect by studying the cases from $L = 300$ to $L = 10\,000$ sites, and is not sensitive to harmonic trapping potentials in real experiments [47].

Finally, let us discuss the experimental relevant time-scales, namely, the decoherence time τ_ϕ ($\sim 1/\eta$) [64] related

to the cavity loss, the cavity-mediated long-range interaction time $1/U_1$ with $U_1 = [(\eta^2 \tilde{\Delta}_c)/(\tilde{\Delta}_c^2 + \kappa^2)]$ [61], and the localization timescale $1/J \sim 1/\chi$. In the vicinity of the superradiant instability, as focused here, we have $\eta/J \rightarrow 0$ such that $\{\tau_\phi, 1/U_1\} \gg 1/J$, for which the decoherence and long-range interacting effects are not important for the localization driven superradiant instability.

In conclusion, we have predicted theoretically a novel superradiant instability by coupling the BEC in a localized phase to the cavity, in which the optical pumping threshold for the superradiance vanishes. The localization drives the resonant superradiant scattering, in sharp contrast to the extended phases, for which the superradiance phase can occur at a vanishing pumping strength. The prediction is well accessible in the current experiments, and is expected to be valid in the many-body localization regime [57–60] which is achieved when the interaction between atoms is included. This study can open up an intriguing avenue in bridging the studies on the Dicke superradiance and the Anderson localization, as well as the many-body localization.

We acknowledge N. R. Cooper and H. Zhai for helpful discussions. This work is supported by the National Natural Science Foundation of China (11875195, 11404225, 11825401, 11474205, 11504037, 11761161003, 11921005), National Key R&D Program of China (2016YFA0301604), the Research Council (Grant No. MIP-086/2015), and the Strategic Priority Research Program of Chinese Academy of Science (Grant No. XDB28000000). Q. S. and A.-C. J. also acknowledge the support by the foundation of Beijing Education Committees under Grants No. CIT&TCD201804074 and No. KZ201810028043.

* andrewjee@sina.com

† gediminas.juzeliunas@tfai.vu.lt

‡ xiongjunliu@pku.edu.cn

§ sunqing@cnu.edu.cn

- [1] P. Domokos and H. Ritsch, *J. Opt. Soc. Am. B* **20**, 1098 (2003).
- [2] J. K. Asbóth, P. Domokos, H. Ritsch, and A. Vukics, *Phys. Rev. A* **72**, 053417 (2005).
- [3] D. Nagy, J. K. Asbóth, P. Domokos, and H. Ritsch, *Europhys. Lett.* **74**, 254 (2006).
- [4] I. B. Mekhov, C. Maschler, and H. Ritsch, *Nat. Phys.* **3**, 319 (2007).
- [5] F. Brennecke, T. Donner, S. Ritter, T. Bourdel, M. Köhl, and T. Esslinger, *Nature (London)* **450**, 268 (2007).
- [6] Y. Colombe, T. Steinmetz, G. Dubois, F. Linke, D. Hunger, and J. Reichel, *Nature (London)* **450**, 272 (2007).
- [7] D. Nagy, G. Szirmai, and P. Domokos, *Eur. Phys. J. D* **48**, 127 (2008).
- [8] H. Ritsch, P. Domokos, F. Brennecke, and T. Esslinger, *Rev. Mod. Phys.* **85**, 553 (2013).
- [9] I. B. Mekhov and H. Ritsch, *J. Phys. B* **45**, 102001 (2012).
- [10] J. Larson, B. Damski, G. Morigi, and M. Lewenstein, *Phys. Rev. Lett.* **100**, 050401 (2008); J. Larson, S. Fernández-Vidal, G. Morigi, and M. Lewenstein, *New J. Phys.* **10**, 045002 (2008).
- [11] S. Gopalakrishnan, B. L. Lev, and P. M. Goldbart, *Nat. Phys.* **5**, 845 (2009); *Phys. Rev. A* **82**, 043612 (2010); *Phys. Rev. Lett.* **107**, 277201 (2011).
- [12] P. Strack and S. Sachdev, *Phys. Rev. Lett.* **107**, 277202 (2011); M. Müller, P. Strack, and S. Sachdev, *Phys. Rev. A* **86**, 023604 (2012).
- [13] F. Brennecke, S. Ritter, T. Donner, and T. Esslinger, *Science* **322**, 235 (2008).
- [14] D. Nagy, G. Kónya, G. Szirmai, and P. Domokos, *Phys. Rev. Lett.* **104**, 130401 (2010).
- [15] S. Gupta, K. L. Moore, K. W. Murch, and D. M. Stamper-Kurn, *Phys. Rev. Lett.* **99**, 213601 (2007); K. W. Murch, K. L. Moore, S. Gupta, and D. M. Stamper-Kurn, *Nat. Phys.* **4**, 561 (2008).
- [16] J. Keeling, M. J. Bhaseen, and B. D. Simons, *Phys. Rev. Lett.* **105**, 043001 (2010).
- [17] R. Kanamoto and P. Meystre, *Phys. Rev. Lett.* **104**, 063601 (2010).
- [18] Q. Sun, X.-H. Hu, W. M. Liu, X. C. Xie, and A.-C. Ji, *Phys. Rev. A* **84**, 023822 (2011); Q. Sun, W. M. Liu, and A.-C. Ji, *New J. Phys.* **15**, 013013 (2013).
- [19] B. Padhi and S. Ghosh, *Phys. Rev. Lett.* **111**, 043603 (2013).
- [20] R. Landig, L. Hruby, N. Dogra, M. Landini, R. Mottl, T. Donner, and T. Esslinger, *Nature (London)* **532**, 476 (2016).
- [21] A. U. J. Lode and C. Bruder, *Phys. Rev. Lett.* **118**, 013603 (2017).
- [22] R. H. Dicke, *Phys. Rev.* **93**, 99 (1954).
- [23] F. Dimer, B. Estienne, A. S. Parkins, and H. J. Carmichael, *Phys. Rev. A* **75**, 013804 (2007).
- [24] K. Baumann, C. Guerlin, F. Brennecke, and T. Esslinger, *Nature (London)* **464**, 1301 (2010).
- [25] K. Baumann, R. Mottl, F. Brennecke, and T. Esslinger, *Phys. Rev. Lett.* **107**, 140402 (2011).
- [26] R. Mottl, F. Brennecke, K. Baumann, R. Landig, T. Donner, and T. Esslinger, *Science* **336**, 1570 (2012).
- [27] F. Brennecke, R. Mottl, K. Baumann, R. Landig, T. Donner, and T. Esslinger, *Proc. Natl. Acad. Sci. U.S.A.* **110**, 11763 (2013).
- [28] J. Léonard, A. Morales, P. Zupancic, T. Esslinger, and T. Donner, *Nature (London)* **543**, 87 (2017).
- [29] F. Mivehvar, H. Ritsch, and F. Piazza, *Phys. Rev. Lett.* **123**, 210604 (2019).
- [30] J. Keeling, M. J. Bhaseen, and B. D. Simons, *Phys. Rev. Lett.* **112**, 143002 (2014).
- [31] F. Piazza and P. Strack, *Phys. Rev. Lett.* **112**, 143003 (2014).
- [32] Y. Chen, Z. Yu, and H. Zhai, *Phys. Rev. Lett.* **112**, 143004 (2014).
- [33] J.-S. Pan, X.-J. Liu, W. Zhang, W. Yi, and G.-C. Guo, *Phys. Rev. Lett.* **115**, 045303 (2015).
- [34] D. Yu, J.-S. Pan, X.-J. Liu, W. Zhang, and W. Yi, *Front. Phys.* **13**, 136701 (2018).
- [35] M. R. Bakhtiari, A. Hemmerich, H. Ritsch, and M. Thorwart, *Phys. Rev. Lett.* **114**, 123601 (2015).
- [36] J. Klinder, H. Keßler, M. R. Bakhtiari, M. Thorwart, and A. Hemmerich, *Phys. Rev. Lett.* **115**, 230403 (2015).

- [37] J. Klinder, H. Keßler, M. Wolke, L. Mathey, and A. Hemmerich, *Proc. Natl. Acad. Sci. U.S.A.* **112**, 3290 (2015).
- [38] W. Zheng and N. R. Cooper, *Phys. Rev. Lett.* **117**, 175302 (2016).
- [39] Y. Chen, Z. Yu, and H. Zhai, *Phys. Rev. A* **93**, 041601(R) (2016).
- [40] N. Dogra, F. Brennecke, S. D. Huber, and T. Donner, *Phys. Rev. A* **94**, 023632 (2016).
- [41] H. Habibian, A. Winter, S. Paganelli, H. Rieger, and G. Morigi, *Phys. Rev. Lett.* **110**, 075304 (2013).
- [42] L. Zhou, H. Pu, K. Zhang, X.-D. Zhao, and W. Zhang, *Phys. Rev. A* **84**, 043606 (2011).
- [43] K. Rojan, R. Kraus, T. Fogarty, H. Habibian, A. Minguzzi, and G. Morigi, *Phys. Rev. A* **94**, 013839 (2016).
- [44] W. Zheng and N. R. Cooper, *Phys. Rev. A* **97**, 021601(R) (2018).
- [45] S. Aubry and G. André, *Ann. Isr. Phys. Soc.* **3**, 133 (1980).
- [46] G. Roati, C. D'Errico, L. Fallani, M. Fattori, C. Fort, M. Zaccanti, G. Modugno, M. Modugno, and M. Inguscio, *Nature (London)* **453**, 895 (2008).
- [47] E. E. Edwards, M. Beeler, T. Hong, and S. L. Rolston, *Phys. Rev. Lett.* **101**, 260402 (2008).
- [48] Y. Lahini, R. Pugatch, F. Pozzi, M. Sorel, R. Morandotti, N. Davidson, and Y. Silberberg, *Phys. Rev. Lett.* **103**, 013901 (2009).
- [49] L. Fallani, J. E. Lye, V. Guarrera, C. Fort, and M. Inguscio, *Phys. Rev. Lett.* **98**, 130404 (2007).
- [50] M. Modugno, *New J. Phys.* **11**, 033023 (2009).
- [51] G. Modugno, *Rep. Prog. Phys.* **73**, 102401 (2010).
- [52] Y. Lahini, Y. Bromberg, D. N. Christodoulides, and Y. Silberberg, *Phys. Rev. Lett.* **105**, 163905 (2010).
- [53] J. Biddle, B. Wang, D. J. Priour, Jr., and S. Das Sarma, *Phys. Rev. A* **80**, 021603(R) (2009).
- [54] J. Biddle and S. Das Sarma, *Phys. Rev. Lett.* **104**, 070601 (2010).
- [55] S. Ganeshan, K. Sun, and S. Das Sarma, *Phys. Rev. Lett.* **110**, 180403 (2013).
- [56] M. Larcher, M. Modugno, and F. Dalfovo, *Phys. Rev. A* **83**, 013624 (2011).
- [57] M. Schreiber, S. S. Hodgman, P. Bordia, H. P. Lüschen, M. H. Fischer, R. Vosk, E. Altman, U. Schneider, and I. Bloch, *Science* **349**, 842 (2015).
- [58] S. Ganeshan, J. H. Pixley, and S. Das Sarma, *Phys. Rev. Lett.* **114**, 146601 (2015).
- [59] H. P. Lüschen, S. Scherg, T. Kohlert, M. Schreiber, P. Bordia, X. Li, S. Das Sarma, and I. Bloch, *Phys. Rev. Lett.* **120**, 160404 (2018).
- [60] X. Li, X. Li, and S. Das Sarma, *Phys. Rev. B* **96**, 085119 (2017).
- [61] See Supplemental Material at <http://link.aps.org/supplemental/10.1103/PhysRevLett.124.113601> for the derivation of the cavity-mediated long-range interaction and the self-consistent atomic density distributions, which includes Refs. [62,63].
- [62] P. Sierant, K. Biedroń, G. Morigi, and J. Zakrzewski, *SciPost Phys.* **7**, 008 (2019).
- [63] N. Ng and M. Kolodrubetz, *Phys. Rev. Lett.* **122**, 240402 (2019).
- [64] Y. Imry, *Introduction to Mesoscopic Physics* (Oxford University Press, Oxford, 1997), Chap. 3.